Structural transformations of carbon chains inside nanotubes

Jamie H. Warner,[1,*] Mark H. Rümmeli,[2] Alicja Bachmatiuk,[2] and Bernd Büchner[2]
[1]*Department of Materials, University of Oxford, Parks Road, Oxford OX1 3PH, United Kingdom*
[2]*IFW Dresden, P.O. Box 270116, D-01171 Dresden, Germany*
(Received 11 November 2009; revised manuscript received 20 January 2010; published 7 April 2010)

In situ aberration-corrected high-resolution transmission electron microscopy is used to examine the structural transformations of carbon chains that occur in the interior region of carbon nanotubes. We find electron-beam irradiation leads to the formation of two-dimensional carbon structures that are freely mobile inside the nanotube. The inner diameter of the nanotube influences the structural transformations of the carbon chains. As the diameter of the nanotube increases, electron-beam irradiation leads to curling of the chains and eventually the formation of closed looped structures. The closed looped structures evolve into spherical fullerenelike structures that exhibit translational motion inside the nanotubes and also coalesce to form larger nanotube structures. These results demonstrate the use of carbon nanotubes as test tubes for growing small carbon nanotubes within the interior by using only electron-beam irradiation at 80 kV.

DOI: 10.1103/PhysRevB.81.155419 PACS number(s): 61.48.De, 61.46.−w, 61.80.Fe

I. INTRODUCTION

The formation of sp^2 carbon-based nanostructures often requires elevated temperatures and this makes it challenging to conduct *in situ* monitoring of the growth process using imaging techniques. Some success has been achieved to image the growth of carbon nanotubes using transmission electron microscopes equipped with an environmental holder.[1] However, it is difficult to obtain sufficient resolution to image the atomic structure of the carbon atoms.[2] The interior space inside carbon nanotubes offers a confined environment for reactions to occur.[3,4] It also provides an ideal sample holder for directly imaging the atomic structure of molecules using high-resolution transmission electron microscopy (HRTEM).[5,6] These two attributes can be combined to enable the *in situ* monitoring of reactions inside carbon nanotubes driven by energy supplied by electron-beam irradiation.[7,8]

This technique has been successful in revealing the detailed structural transformations that occur during the coalescence of endohedral fullerenes,[9–13] the enlargement of a fullerene through the interaction with metal atoms,[14] the passage of molecules through nanopores,[15] and the motional dynamics of small organic molecules.[16] The electron-beam-induced formation of fullerenelike cages and closed graphitic structures have been observed using transmission electron microscopy with high accelerating voltages between 400 and 1250 kV.[17,18] When the accelerating voltage of the electrons is high (i.e., >160 kV), knock-on structural damage is expected to occur for graphitic systems.[19] This threshold is lowered for graphitic systems with curvature such as nanotubes and fullerenes, where bond strain is induced.[20] We have shown that under certain conditions, electron-beam irradiation at 80 kV can induce reactions within the nanotube without distorting its structure.[13]

Here we show how electron-beam irradiation at a low accelerating voltage of 80 kV can be used to fabricate small carbon nanostructures inside carbon nanotubes. We study the structural transformations *in situ* and reveal how they are influenced by the diameter of the inner nanotube. We show that carbon chains can form closed looped structures, which can also fuse together to form larger structures inside the original nanotube host. These results demonstrate the rich activity of carbon species confined to the interior of carbon nanotubes and how electron-beam irradiation leads to the formation of unique nanostructures.

II. EXPERIMENTAL METHODS

Double-walled carbon nanotubes (DWNTs) (Helix) and triple-walled carbon nanotubes (TWNTs) (Helix) were used for the electron-beam irradiation studies due to their superior strength and stability against damage as compared to single-walled carbon nanotubes. The nanotubes were annealed in air at 420 °C for 1 h in order to open the end caps. This also ensures that any adsorbents such as oil, grease, gas, and water are removed. This enables us to preclude these contaminants from our observations. The nanotubes were then sealed under vacuum and annealed at 450 °C for 4 days to encourage atomic and molecular carbon species to enter inside the nanotubes. The nanotubes were then dispersed in methanol via sonication and deposited onto lacey carbon-coated TEM grids. HRTEM was performed using a FEI Titan^3 operating at 80 kV with spherical aberration correction. A constant electron-beam current density was used and estimated to be between 0.01 and 0.1 pA/nm^2.

III. RESULTS AND DISCUSSION

A. *In situ* evolution of linear carbon chains inside a nanotube with narrow diameter

We found an appreciable amount of material encapsulated inside the nanotubes. In particular, larger 2–3 nm diameter nanotubes contained amorphous aggregates. We chose to examine narrow diameter DWNTs and TWNTs because of the restricted volume their interior possess, which leads to confinement of the encapsulated species. Figure 1 shows a time series of HRTEM images, with 2 s between frames, of a linear carbon chain inside a DWNT. The carbon chain occupies only part of the DWNT, indicated with the dotted white brackets, and gives rise to increased contrast in the central

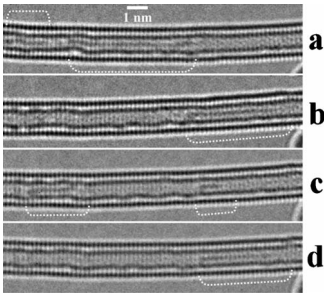

FIG. 1. Time series (a)–(d) of HRTEM images showing the motion of a linear carbon chain inside a DWNT. Time between frames is 2 s.

region. The length of the linear carbon chains ranged from 1 to 6 nm. The position of the carbon chain can be seen to move between frames, indicating that the chain is mobile within the DWNT. The mobility of the carbon chain is possibly driven by energy supplied by the 80 kV electron-beam irradiation in the form of electron-beam-induced charging. The energy barrier for movement within the DWNT may be low enough that the motion occurs at room temperature and is intrinsic to the system. Heating of carbon nanotubes from electron-beam irradiation is generally expected to be minimal.

B. HRTEM simulation of linear carbon chains

Zhao *et al.* have reported the observation of novel carbon nanowires formed from long linear carbon chains inside multiwalled carbon nanotubes (MWNTs).[21] The carbon nanowires were identified by imaging with HRTEM. HRTEM imaging of MWNTs can lead to the appearance of a line in the central region of the MWNT, which may give rise to misleading results and therefore comparison with image simulations is important. The linear carbon chains observed in Fig. 1 may not necessarily be monatomic (i.e., one atom thick). In order to interpret our HRTEM images in Fig. 1, we performed multislice HREM image simulations using JEMS software. Supercells (5 nm$\times$2 nm$\times$2 nm) were constructed around a DWNT with (19,0) outer chirality and (9,0) inner chirality. Defocus spread was set to 5.6 nm and C_s set to −0.02 mm. Six different filling scenarios were investigated and the respective atomic structural models are shown in Fig. 2(i) for (a) empty, (b) alkane chain, (c) alkane chain rotated 90°, (d) linear chain of benzene rings, (e) linear chain of benzene rings rotated 90°, and (f) polyyne chain. In Fig. 2, image simulations were generated for defocus values of (ii) 0 nm, (iii) 5 nm, (iv) 10 nm, and (v) 15 nm. Figures 2(a)(ii)–2(a)(v) show that even for an empty DWNT, a line of contrast is observed in the central region. The image simulations for the DWNT filled with linear carbon chains show an increase in the contrast over the region where they are located. The ends of the linear chains can be identified, highlighting the ability to determine filled and empty regions within the same DWNT. When the defocus increases to 15 nm, the images become blurred and the contrast reduces. The lowest contrast occurs for the linear chain of benzene rings in Figs. 2(d)(ii)–2(d)(v). However, when rotated 90°, Figs. 2(e)(ii)–2(e)(v), the contrast increases substantially. The image simulations in Fig. 2 show that even small linear carbon chains such as a polyyne chain or linear alkane give rise to appreciable contrast in HRTEM and permit their detection inside DWNTs.

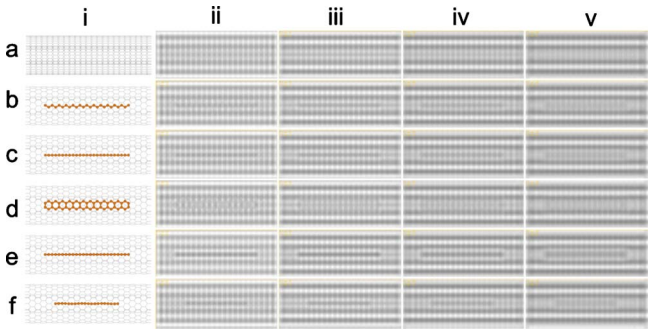

FIG. 2. (Color online) (i) Atomic structural model of the supercells used for HREM image simulations of a (19,0) outer chirality and (9,0) inner chirality DWNT with six different filling scenarios (a) empty, (b) alkane chain, (c) alkane chain rotated 90°, (d) linear chain of benzene rings, (e) linear chain of benzene rings rotated 90°, and (f) polyyne chain. HREM image simulations are shown to the right of each structural model in (i) with defocus values of (ii) 0 nm, (iii) 5 nm, (iv) 10 nm, and (v) 15 nm.

C. *In situ* evolution of carbon chains inside a nanotube with a larger diameter

The narrow diameter (0.7 nm) of the inner nanotube in Fig. 1 provides a restricted space that forces the carbon chain to remain linear and exhibit one-dimensional confined motion along the nanotube axis. However, we observed different behavior when the diameter of the inner nanotube increased. Figure 3(i) shows a time series of HRTEM images of a carbon chain inside a TWNT with an inner diameter of 1.4 nm. The time between frames is 2 s. Figure 3(i)(a) shows a carbon chain, having sufficient room inside the nanotube to curl up. Figure 3(i)(b) shows that after 2 s of electron-beam irradiation, the chain has extended out and its top end is in contact with the inner wall of the nanotube. In Fig. 3(i)(c), the top of the chain has become detached from the inner tube. The other end of the chain becomes attached to the inner tube in Fig. 3(i)(d). In Fig. 3(i)(e), the chain is detached again and has curled up significantly. Finally by Fig. 3(i)(h), the ends of the chain have joined each other to form a closed-loop structure. Figures 3(ii) and 3(iii) show similar cases of linear carbon chains curling up to form closed-loop structures within (ii) a TWNT and (iii) a DWNT, showing that this phenomena is repeatedly observed in our experimental setup.

These results show that carbon chains are dynamic inside the larger 1.4 nm nanotube interior and electron-beam irradiation can lead to the formation of closed looped structures. We found that once the closed-loop structures formed, they were very stable and did not revert back to the linear configuration. The end of the carbon chain is likely to contain unsaturated atoms that are reactive. When the two ends of the carbon chain meet, it is possible that they covalently

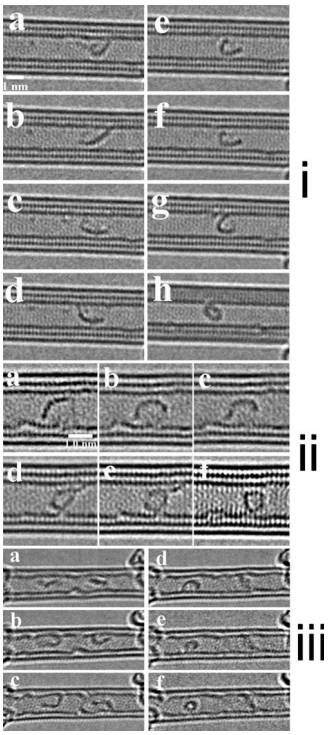

FIG. 3. Three examples [(i), (ii), and (iii)] of time series of HRTEM images showing the dynamics of a carbon chains under electron-beam irradiation. Time between frames is 2 s.

bond to form a stable structure. This is different to the case when the end of the carbon chain comes in contact with the nanotube wall. Carbon atoms within the nanotube's walls have sp^2 bonding and are saturated and stable. The curvature of the nanotube causes the π orbitals to extend further toward the outer side of the nanotube and reduces the overlap within the interior of the nanotube. The end of a carbon chain may interact via van der Waals forces with the nanotube wall but unless a defect is present, direct covalent bonding may not occur. This then allows the carbon chain to attach and detach itself from the nanotube wall intermittently.

If the structures were to remain as simple rings then as they rotate inside the nanotube, the apparent cross section observed would change and in some cases should appear with linear or rectangular profile. Instead we found the structures retained their round cross section and this suggests they have evolved into spherical fullerenelike structures. Figure 4(i)(a) shows the same structure as in Fig. 3(iii)(f) after a further 30 s of electron-beam irradiation, confirming the structures maintain their round cross section and are spherical. Further confirmation that the structures are spherical can be obtained by examining the changes in apparent cross sectional after translational motion. The spherical structures displayed sporadic motion inside the nanotube, similar to the behavior of fullerenes under electron-beam irradiation.[22] The HRTEM image in Fig. 4(i)(b) was taken 10 s after Fig. 4(i)(a) and shows the fullerenelike structure has moved slightly toward the right-hand side and yet still maintains its round cross section. Figure 4(ii) shows two HRTEM images of a spherical fullerenelike structure formed by electron-beam irradiation with 10 s between Figs. 4(ii)(a) and 4(ii)(b).

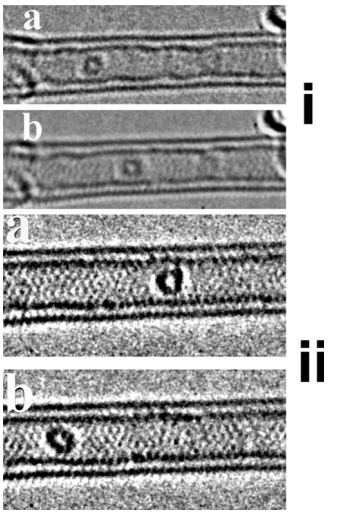

FIG. 4. (i) TEM image of the same round structure as in Fig. 3(iii)(h) after (a) 30 s and (b) 40 s. (ii) TEM image of a round structure formed by electron-beam irradiation (a) before and (b) after 10 s.

During this time, the fullerene has moved an appreciable distance toward the left. Figure 4 demonstrates that even after translational motion, the structures formed by electron-beam irradiation retain their round cross section and this confirms their three-dimensional (3D) spherical geometry. Carbon atoms and small clusters of carbon atoms may migrate along the interior of the nanotube and eventually attach to the closed ring structures to provide the extra material that enables them to evolve into a spherical fullerene. Evidence of such migration can be seen in Fig. 3(i)(c), where two spots with strong contrast are apparent, and are attributed to either a single or small cluster of carbon atoms (i.e., 1–5). By Fig. 3(i)(h), these two spots of strong contrast have gone, indicating the carbon clusters can move within the interior region of the nanotube.

In order to form the fullerenelike structures observed in Figs. 3 and 4, both five-member and six-member rings with sp^2 bonding should be present. Five-member carbon rings are the essential component that enables fullerenes to form spherical structures and the end caps of carbon nanotubes to also be hemispherical. Figure 3 shows that fullerene formation occurs via the addition of small carbon clusters to a longer linear-chain structure and not through the addition of several medium sized chains. Figures 5(i)(a)–5(i)(g) show a sequence of atomic structural models demonstrating the idealized transformation of a linear carbon chain consisting of five-member and six-member rings into a C_{60} fullerene. The linear chain gradually curls up to form a closed-loop structure, Fig. 5(i)(e), upon which further carbon atoms are added to the side to form a C_{60} fullerene, Fig. 5(i)(g). The initial starting linear chains in our HRTEM observations most likely deviate slightly from the idealized structure presented in Fig. 5(i) with different arrangements of the five- and six-member rings and consequently not necessary lead to C_{60}. However, Fig. 5(i) illustrates how a linear carbon chain may evolve into a spherical fullerene structure.

Image simulations were performed for four different types of fillings in a TWNT in order to examine the difference in

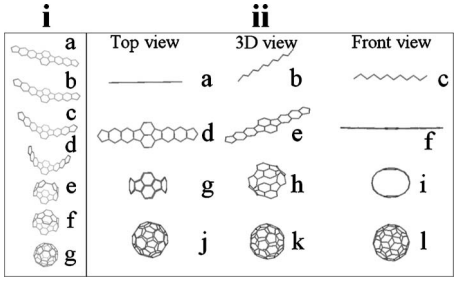

FIG. 5. (i) Sequence (a)–(g) of atomic structural models demonstrating the idealized transformation of a linear carbon chain consisting of five-member and six-member rings into a fullerene. (ii) Atomic structural models for an alkane chain with (a) top view (TV), (b) 3D view (3D), (c) front view (FV), linear carbon chain comprised of five-member and six-member rings with (d) TV, (e) 3D, and (f) FV, closed loop with (g) TV, (h), 3D, and (i) FV, and C60 with (j) TV, (k) 3d, and (l) FV.

contrast from a closed-loop structure as compared to a C_{60} fullerene. Figure 5(ii) shows the atomic structural models for an alkane chain with (a) top view (TV), (b) 3D view (3D), and (c) front view (FV), linear carbon chain comprised of five-member and six-member rings with (d) TV, (e) 3D, and (f) FV, closed loop formed in Fig. 5(i)(f) with (g) TV, (h) 3D, and (i) FV, and C_{60} with (j) TV, (k) 3D, and (l) FV. For the image simulations, the structures are placed inside a TWNT with front-view projection. The TWNT has a (19, 0) inner tube with $d=1.49$ nm, (20,8) middle tube with $d=1.96$ nm, and (20,16) outer tube with $d=2.45$ nm. Figure 6 shows the image simulations for defocus values of (i) 0 nm, (ii) 5 nm, (iii) 10 nm, and (iv) 15 nm for (a) empty TWNT, (b) TWNT filled with an alkane chain, (c) TWNT filled with a linear carbon chain comprised of a five-member and six-member rings, (d) TWNT filled with a closed-loop structure, and (e) TWNT filled with C_{60}. For the case of 0 nm defocus, mini-

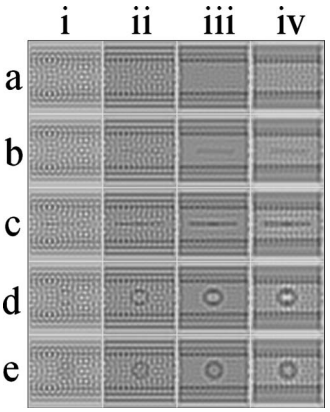

FIG. 6. Image simulations with defocus values of (i) 0 nm, (ii) 5 nm, (iii) 10 nm, and (iv) 15 nm for (a) empty TWNT with a (19,0) inner tube with $d=1.49$ nm, (20,8) middle tube with $d=1.96$ nm, and (20,16) outer tube with $d=2.45$ nm. (b) TWNT filled with an alkane chain shown in Fig. 5(ii)(c), (c) TWNT filled with carbon chain comprised of five-member and six-member rings shown in Fig. 5(ii)(f), (d) TWNT filled with a closed-loop carbon chain shown in Fig. 5(ii)(i) and (d) TWNT filled with C_{60} shown in Fig. 5(ii)(l).

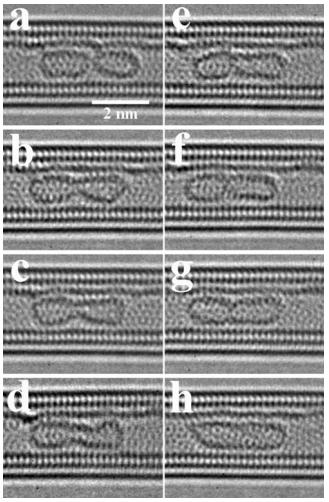

FIG. 7. Time series of HRTEM images (a)–(h) showing the fusion of two spherical fullerenelike structures into one larger structure inside a TWNT.

mal contrast is observed from the encapsulated materials in nearly all cases. For a defocus of 10 nm, contrast from the encapsulated material is strong and the walls of the TWNT are still resolved. For a defocus of 15 nm, the walls of the TWNT are no longer resolved. A comparison can be made between the contrast of the inner wall and the encapsulated material for a defocus of 10 nm, with the alkane chain having less contrast than the inner TWNT wall, Fig. 6(iii)(b) while Figs. 6(iii)(c)–6(iii)(e) all show similar contrast to the inner TWNT wall. The HRTEM images presented in Fig. 3 show the carbon chains have similar contrast to the inner wall of the TWNT and thus our image simulations tend to suggest that these structures are not single chain alkanes but rather chains which are two or more atoms thick as presented in Fig. 6(iii)(c). This supports the notion that chains comprised of five- and six-member rings are formed within the TWNT and curl up to form closed-loop structures and eventually fullerenes.

D. Coalescence of spherical fullerenelike structures into larger structures inside the nanotube

Prolonged electron-beam irradiation led to the formation of larger fullerenelike and nanotubelike structures. These were formed by the coalescence of smaller spherical structures as they migrate within the interior of the nanotube, similar to fullerene coalescence in peapods.[12] Figure 7 shows a time series of HRTEM images capturing the fusion of two spherical fullerenelike structures into one larger structure. The time between images is 10 s. In Fig. 7(a), two elongated oval-shaped fullerene structures are observed. These two structures were formed from carbon chains using electron-beam irradiation, similar to the process shown in Fig. 3. In Fig. 7(b), the two structures have started to coalesce. In Fig. 7(d), the two structures have fused into one and by Fig. 7(h), the electron-beam irradiation has enabled the structure to reconfigure itself into a small nanotube. This sequence of images provides strong evidence for the formation of 3D structures within the TWNT host.

IV. CONCLUSION

The results presented in Figs. 1–7, demonstrate how electron-beam irradiation can lead to reactions between carbon atoms inside a nanotube. The formation of 3D spherical structures of carbon typically requires both five-member and six-member carbon rings and our image simulations of such structures match well with experimental observations. The restricted volume of the interior of the nanotube provides an ideal space to conduct reactions and by changing the diameter of nanotube, different reaction pathways are opened up. This led to the formation of closed-loop structures, which evolved into fullerenes and then small nanotubes. This approach is nondestructive and may be used to alter the structure of carbon nanotubes on the nanoscale.

ACKNOWLEDGMENTS

J.H.W. thanks the Violette and Samuel Glasstone Fund, and Brasenose College, Oxford for support.

*jamie.warner@materials.ox.ac.uk

[1] H. Yoshida, S. Takeda, T. Uchiyama, H. Kohno, and Y. Homma, Nano Lett. **8**, 2082 (2008).
[2] H. Yoshida and S. Takeda, Phys. Rev. B **72**, 195428 (2005).
[3] D. A. Britz, A. N. Khlobystov, K. Porfyrakis, A. Ardavan, and G. A. D. Briggs, Chem. Commun. (Cambridge) **2005**, 37.
[4] R. Pfeiffer, M. Holzweber, H. Peterlik, H. Kuzmany, Z. Liu, K. Suenaga, and H. Kataura, Nano Lett. **7**, 2428 (2007).
[5] Z. Liu, K. Yanagi, K. Suenaga, H. Kataura, and S. Iijima, Nat. Nanotechnol. **2**, 422 (2007).
[6] Y. Sato, K. Suenaga, S. Okubo, T. Okazaki, and S. Iijima, Nano Lett. **7**, 3704 (2007).
[7] A. Chuvilin, A. N. Khlobystov, D. Obergfell, M. Haluska, S. Yang, S. Roth, and U. Kaiser, Angew. Chem. **49**, 193 (2010).
[8] M. Koshino, Y. Niimi, E. Nakamura, H. Kataura, T. Okazaki, K. Suenaga, and S. Iijima, Nat. Chem. (to be published).
[9] K. Urita, Y. Sato, K. Suenaga, A. Gloter, A. Hashimoto, M. Ishida, T. Shimada, H. Shinohara, and S. Iijima, Nano Lett. **4**, 2451 (2004).
[10] T. Okazaki, K. Suenaga, K. Hirahara, S. Bandow, S. Iijima, and H. Shinohara, J. Am. Chem. Soc. **123**, 9673 (2001).
[11] E. Hernández, V. Meunier, B. W. Smith, R. Rurali, H. Terrones, M. Buongiorno Nardelli, M. Terrones, D. E. Luzzi, and J.-C. Charlier, Nano Lett. **3**, 1037 (2003).
[12] J. H. Warner, Y. Ito, M. Zaka, L. Ge, T. Akachi, H. Okimoto, K. Porfyrakis, A. A. R. Watt, H. Shinohara, and G. A. D. Briggs, Nano Lett. **8**, 2328 (2008).
[13] J. H. Warner, Y. Ito, M. H. Ruemmeli, T. Gemming, B. Buechner, H. Shinohara, and G. A. D. Briggs, Phys. Rev. Lett. **102**, 195504 (2009).
[14] C. Jin, H. Lan, K. Suenaga, L.-M. Peng, and S. Iijima, Phys. Rev. Lett. **101**, 176102 (2008).
[15] M. Koshino, N. Solin, T. Tanaka, H. Isobe, and E. Nakamura, Nat. Nanotechnol. **3**, 595 (2008).
[16] M. Koshino, T. Tanaka, N. Solin, K. Suenaga, H. Isobe, and E. Nakamura, Science **316**, 853 (2007).
[17] A. P. Burden and J. L. Hutchinson, J. Cryst. Growth **158**, 185 (1996).
[18] T. Füller and F. Banhart, Chem. Phys. Lett. **254**, 372 (1996).
[19] F. Banhart, Rep. Prog. Phys. **62**, 1181 (1999).
[20] A. V. Krasheninnikov and F. Banhart, Nature Mater. **6**, 723 (2007).
[21] X. Zhao, Y. Ando, Y. Liu, M. Jinno, and T. Suzuki, Phys. Rev. Lett. **90**, 187401 (2003).
[22] B. W. Smith, M. Monthioux, and D. E. Luzzi, Chem. Phys. Lett. **315**, 31 (1999).